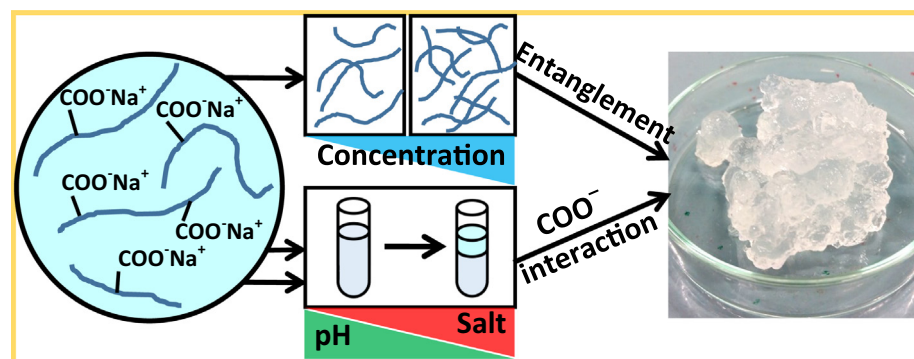


Regular Article

Gelation mechanism of cellulose nanofibre gels: A colloids and interfacial perspective

Llyza Mendoza^a, Warren Batchelor^a, Rico F. Tabor^b, Gil Garnier^{a,*}^a Bioresource Processing Research Institute of Australia (BioPRIA), Department of Chemical Engineering, Monash University, VIC 3800, Australia^b School of Chemistry, Monash University, VIC 3800, Australia

GRAPHICAL ABSTRACT



ARTICLE INFO

Article history:

Received 23 May 2017

Revised 24 August 2017

Accepted 24 August 2017

Available online 1 September 2017

Keywords:

Nanocellulose

TEMPO-mediated oxidation

Hydrogels

Colloids

Rheology

AFM

ABSTRACT

Hypothesis: Nanocellulose gels form a new category of sustainable soft materials of industrial interest for a wide range of applications. There is a need to map the rheological properties and understand the mechanism which provides the colloidal stability and gelation of these nanofibre suspensions.

Experiments: TEMPO (2,2,6,6-tetramethylpiperidine-1-oxyl)-oxidised cellulose nanofibre gels were investigated at different fibre concentrations, pH and ionic strength. Dynamic and cyclic rheological studies was performed to quantify gel behaviour and properties. Gels were produced at different pH and salt contents to map and understand colloidal stability of the nanocellulose gel.

Findings: Rheology indicates gelation as a transitional state starting at a fibre concentration of 0.1 wt.%. The colloidal stability of the nanocellulose gel network is controlled by pH and salt, whereas fibre concentration mainly dictates the dynamic rheological properties. Decreasing pH and adding salt destabilises the gel network by eluting bound water which is correlated with the decrease in electrostatic repulsion between fibres. The gelation and colloidal stability of these nanocellulose gels is driven by electrostatic forces and the entanglement ability of the fibrous system to overlap.

Crown Copyright © 2017 Published by Elsevier Inc. All rights reserved.

1. Introduction

Cellulose fibrils of nano-scale width – referred to as nanocellulose – can be extracted from plants and bacterial sources through a variety of mechanical and chemical methods [1,2]. Nanocellulose exhibits exceptional characteristics such as high tensile strength,

* Corresponding author.

E-mail address: gil.garnier@monash.edu (G. Garnier).

ease of functionalisation, combined with its expected biological characteristics: renewability, biocompatibility, biodegradability and low toxicity [3–5]. Isogai et al. developed the TEMPO-mediated oxidation process which utilises a nitroxyl catalyst (TEMPO, 2,2,6,6-tetramethylpiperidine-1-oxyl) to convert the primary alcohol groups of the cellulose D-glucose units into carboxylate groups. This provides the necessary electrostatic repulsion which allows the liberation of nanocellulose fibres [6–8]. TEMPO-oxidised cellulose nanofibres (TOCNFs) macroscopically appear as viscous and stable colloidal suspensions even at low solids content (1–2 wt.%) [9]. This surface modification produces nanofibres 3–4 nm in width and several microns in length [8,10] and is currently considered among the most effective methods for producing nanocellulose [11]. Recent TOCNF studies have focussed on biomedical applications such as drug delivery [12], wound dressing [13], tissue engineering substrate [14] and cell encapsulation [15,16], engineering reinforcement materials in plastics and paper [17–20], rheology modifier [21,22], and the development of novel materials such as aerogels [23]. Previous studies on the properties of TOCNFs investigated the structure at the individual fibril level [24], determining the fibre aspect ratio through rheological measurements [25,26] and modelling properties at the dilute and semi-dilute concentration regimes [26,27]. However, there is poor understanding on what drives the gelation and provides the colloidal stability in TOCNFs. Limited studies have analysed the properties of nanofiber cellulose gels from a colloidal and interfacial perspective.

Polysaccharides, owing to their high degrees of polymerisation and hydrogen bonding ability, can form hydrogels through physical interactions. κ -carrageenan undergoes a coil-to-helix structural transformation as a response to temperature changes and forms gels [28]. Thermo-responsive polysaccharides, which contain methyl or other short hydrophobic groups such as methylcellulose and carboxymethylcellulose, gel through the formation of specific hydrogen bonding combined with hydrophobic associations within the cellulose backbone [29–31]. Alginates, on the other hand, require coordinating cations (i.e. Ca^{2+}) to bridge consecutive alginate polymers which induces gelation [32]. However, none of these gelation mechanisms can describe the gelation of TOCNFs. This type of nanocellulose has been known to form stable gels without the aid of temperature nor cations [27,33]. Although it is recognized that modification of its rheological properties, resulting in stiff and self-standing gels, can be achieved by manipulating pH and the addition of cations [14,34,35].

The objective of this study is to characterise the gelation mechanism of TOCNFs. These fibres, possessing nano-scale diameter and micro-scale length and strong surface charges, can be viewed as flexible colloidal particles of high aspect ratio able to interact, deform and entangle. It is desired to quantify fibre-fibre interactions and determine the factors which affect the stability of the fibres by modifying surface charge and electrical double layer thickness. This is achieved by combining rheology, atomic force microscopy (AFM) and qualitative imaging. Rheology is a well-established method to quantify the viscoelastic characteristics of complex soft materials such as gels. It provides an insight to the state of the gel network by controlled macroscopic deformation [36]. Through rheology, we can monitor the gelation state and properties of TOCNFs as a function of different variables. AFM and light scattering allows the imaging of the cellulose nanofibres enabling us to resolve the fibre dimensions. The combination of these techniques allows us to explore the source of the exceptional colloidal stability and properties of these gels.

To understand the gelation of TOCNFs, we characterised the range of viscoelastic properties in the dilute to semi-dilute range. Their rheological behaviour provides insight into how the fibres organize into a network. The effect of pH and salt on the colloidal

stability of the gels was determined and analysed in terms of colloids and interfacial chemistry. We aim at relating the mechanism of cellulose nanofibre gel properties to the well-established colloid and interface science to efficiently engineer applications in food, biomedical and as rheology modifier.

2. Materials and methods

2.1. Materials

Bleached Eucalyptus Kraft (BEK) pulp of approximately 10 wt.% solids was supplied by Australian Paper, Maryvale, Australia. 2,2,6,6-Tetramethylpiperidine-1-oxyl (TEMPO) and sodium bromide (NaBr) were purchased from Sigma-Aldrich. Hydrochloric acid (HCl) and Sodium Hydroxide (NaOH) were diluted for solutions as required and were purchased from ACL Laboratories and Merck, respectively. 12 w/v% Sodium Hypochlorite (NaClO) was purchased from Thermo Fisher Scientific and used as received.

2.2. TEMPO-mediated oxidation

The TEMPO-mediated oxidation process employed is based on the method of Saito and Isogai [6]. 100 g BEK pulp was suspended in 2500 mL water containing 0.4 g TEMPO and 2.5 g NaBr. The 12 w/v% NaClO solution was initially adjusted to pH 10 via addition of 36% HCl. To initiate the oxidation process, 75 mL NaClO was added drop-wise to the suspension whilst stirred. The pH of the reaction was maintained at 10 through the addition of 0.5 M NaOH. The oxidation process was maintained for 2 h. The oxidised fibres were recovered through filtration and stored refrigerated (4 °C).

The oxidised pulp was then dispersed in deionised water to a desired concentration. Fibrillation was accomplished through a high-pressure homogeniser (GEA Niro Soavi Homogeniser Panda) at 1000 bar. Suspensions which contain less than 1 wt.% TEMPO-oxidised pulp was homogenised for two passes. More concentrated suspensions were homogenised with only one pass. TEMPO-oxidised cellulose nanofibres (TOCNFs) possess an average length of several microns and diameter of 3–4 nm [8,10].

2.3. Determining solids concentration

The solids concentration of all samples (i.e. gel or pulp) were determined through drying. The sample was weighed before (w_i) and after (w_d) drying. Sample moisture was evaporated by drying in an oven at 105° for at least 4 h. The solids content was calculated with:

$$\text{solids content}(\%) = \frac{w_d}{w_i} \times 100\% \quad (1)$$

2.4. Rheology

All rheological testing of the gels were performed with an Anton Paar MCR302 rheometer. A cone (0.997°) and plate (49.975 mm) geometry were selected. Testing was done at ambient temperature (25 °C). To ensure stable temperature during the testing, a solvent trap was used.

Viscosity was measured at shear rate ranging from 0.5 to 100 s^{-1} . Oscillatory strain sweep was performed from 0.01 to 100% at a constant 1 Hz frequency. Frequency sweep was measured from 0.1 to 100 rad/s and at 0.1% strain. All measurements were in triplicates. A thixotropic loop test was performed with a 1 wt.% gel by varying the shear stress between the LVR (0.1%, 1 Hz) and the yielded region (10%, 1 Hz) for 5 cycles.

2.5. Visualising the effect of pH and ionic strength

The effect of pH and salt content on the gel structure was observed qualitatively. The pH of the gels was increased and decreased by adding 0.5 M NaOH and 1 M HCl, respectively. The salt content of the gel was varied between 8.9 mM and 68.5 mM by the addition of 3 M NaCl. The gels were then loaded into test tubes and centrifuged at 4000 rpm for 20 min to separate any released water. The experiment was done in triplicates. Fibre ratio is then calculated as the ratio between the final and initial gel height. The gels were imaged with a black background to enhance visualisation.

2.6. Dynamic light scattering

A DLS measurement (Nanobrook Omni Particle Size Analyser) was performed with a dilute (0.03 wt.%) suspension to estimate fibre length.

2.7. Atomic force microscopy (AFM) imaging

AFM imaging was performed using a JPK Nanowizard 3 to determine fibre diameter and morphology. Samples were prepared by spin coating (Laurell technologies, WS-400BZ-6NPP/LITE) a 0.01 wt.% CNF dispersion onto glass microscope slides. Images were obtained in intermittent contact mode using Brüker NCHV model cantilevers. Due to convolution effects from the finite size of the AFM tip, fibre diameters were obtained from the reported height of single fibres on the surface.

3. Results

3.1. Fibre dimensions and morphology

To characterise the fibre dimensions, atomic force microscopy (AFM) imaging was used, with results shown in Fig. 1. From the

images of spin-coated and dried fibres, it is clear that the fibres are quite monodisperse in diameter, with reported diameters from AFM height measurements of 2–3 nm. Previous reports have shown a similar diameter distribution [8,10]. The fibre lengths are, as expected from previous literature protocols [8,37], more variable and typically the fibres are several microns in length. These fibres have been shown to swell in water depending on their counterion present with the carboxylate pendant group. A Na⁺ counterion was shown to have a higher fibre swelling in contrast to H⁺ [38].

3.2. Effect of pH and ionic strength

The effect of pH and ionic strength on gel is shown in Fig. 2. Varying both variables resulted in the gel losing its homogeneous structure with the formation of heterogeneous clumps in a dilute water matrix. Hence, rheological measurements were not completed due to the phase separation (i.e. release of water) resulting in inaccurate measurements. To visualise the effect of both variables, the gels were placed in tubes and centrifuged to observe any eluted water. Fig. 2A shows the effect of varying the pH of gels. TOCNF gels have an original pH of 7.4. Adding acid (pH<7) increases the amount of water eluted from the gel. The fibres forming the gel become heterogeneously distributed and compact as pH is decreased- indicated by the whitish appearance. However, increasing the pH does not have any observable effects on gel.

Fig. 2B shows the effect of salt concentration on gel stability. The addition of up to 17.4 mM NaCl did not affect nanocellulose gel stability; water is however released over this concentration. The addition of 34.7 mM and 68.5 mM NaCl released increasing amounts of water, respectively. The water released by the gel at the highest salt concentration is comparable to the gel at pH 2.

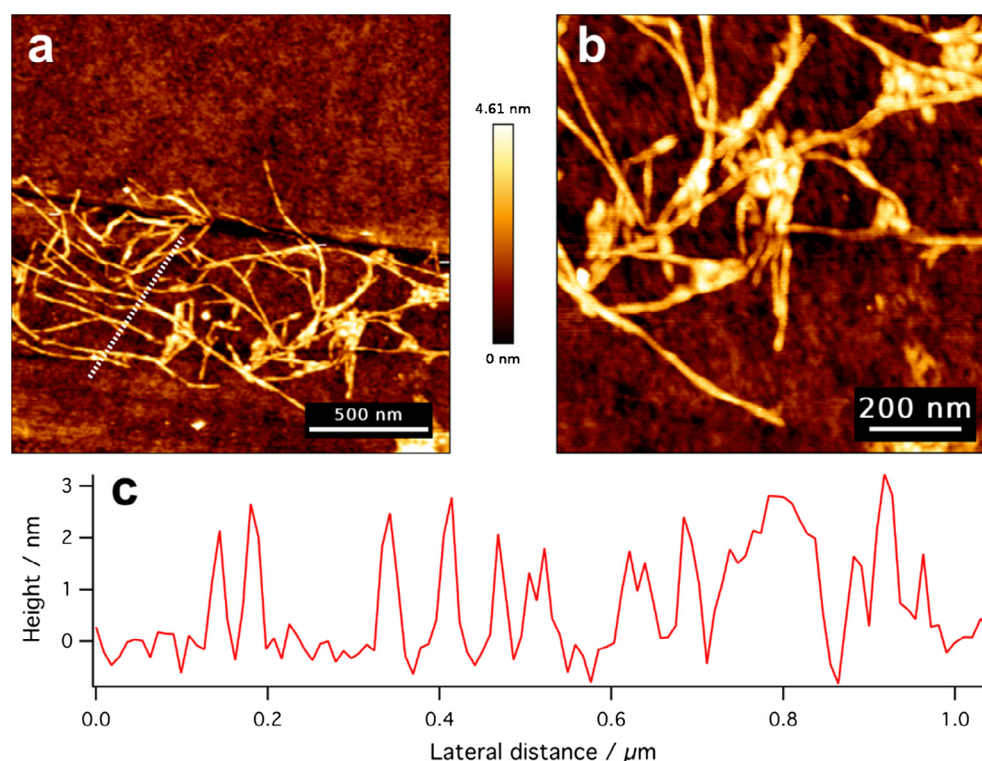


Fig. 1. AFM images of TOCNF spin coated onto a glass slide. (a, b) AFM height images of the fibres at different image sizes. (c) A cross-sectional profile of the surface topology at the point indicated by the white dotted line in (a) showing that the height (diameter) of individual fibres in the dry state is 2–3 nm.

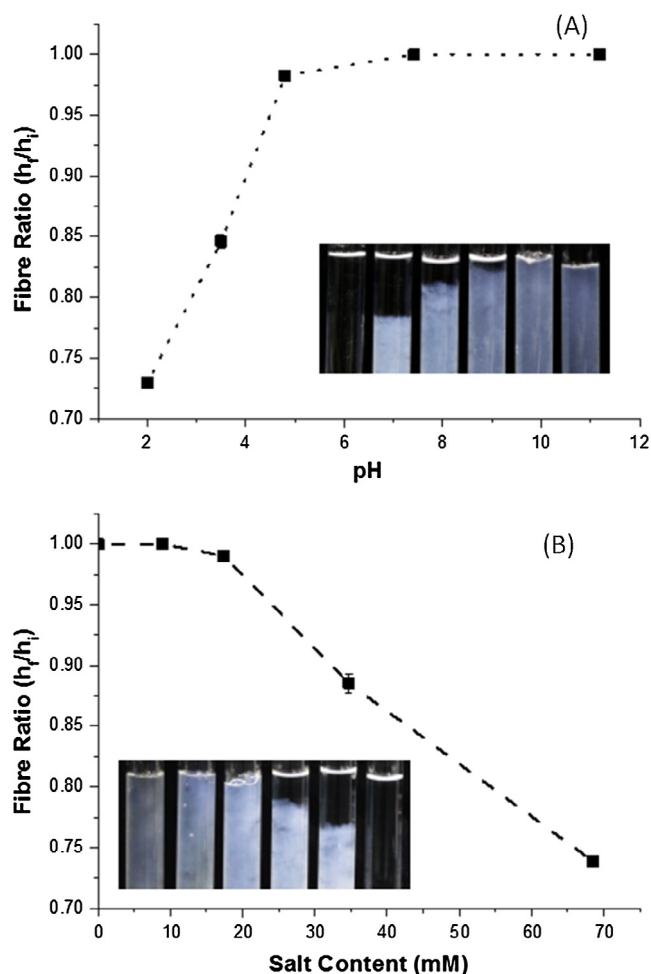


Fig. 2. The effect of (A) pH and (B) salt on the stability of 1 wt.% TEMPO-oxidised cellulose nanofibre gels. Fibre ratio is calculated as the ratio between the final height of gel after centrifugation and the total gel height. Insets show water released from gels at different conditions with pure water as reference.

3.3. Effect of fibre concentration

We measured the effect of fibre concentration on gel properties by rheology. Rheology is an effective method to characterise the behaviour of soft matter such as gels. Rheological measurements can be performed in two modes: steady-shear or oscillatory flow. The effect of shear rate and nanofibre concentration on TOCNF dispersion complex viscosity are presented in Fig. 3. Gel viscosity decreases with shear, denoting shear-thinning behaviour in line with expectation [9,39,40]. Higher zero-shear viscosities are observed with increasing TOCNF concentrations. Gels containing at least 0.29 wt.% TOCNF possess clear yield points, indicating that these are true gels. Indeed, we see some evidence for two yielding zones in the viscosity curves at higher fibre concentrations (discussed later), whereas gels containing less TOCNF (0.09%) have a linearly decreasing viscosity profile.

In oscillatory rheology, the gels are subjected to an increasing oscillating strain (strain sweep) at a constant frequency or vice versa (frequency sweep). In a strain sweep, the range of viscoelastic behaviour can be quantified for gels. The elastic modulus G' describes the solid-like behaviour of TOCNF gel whereas the loss or viscous modulus G'' defines the liquid-like behaviour of the material. Fig. 4 shows the rheological spectra of gels as a function of concentration. At low shear stresses, gels possess a linear viscoelastic region (LVR) wherein the elastic modulus G' and viscous

modulus G'' are independent of the shear stress. Within this region, G' is dominant over G'' , indicating that the material is acting consistently solid-like; elastic behaviour dominates over viscous behaviour. At a critical shear stress, the gel yields as shown by the decrease in G' , and then reaches a “cross-over point” where G'' becomes dominant and the gel begins to flow. Past this critical stress, the viscous regime dominates ($G'' > G'$) indicating that the network structure has yielded and begins to behave as a non-Newtonian shear thinning fluid. Gels containing a fibre content of at least 0.29 wt.% possess a distinct linear viscoelastic region and a yield point. For 0.09 wt.%, the linear viscoelastic region is significantly lengthened, and the cross-over point is not observed in the selected strain range.

The frequency sweep shows the time-dependent behaviour of TOCNF gels at increasing concentrations (Fig. 5). The G' and G'' values are non-intersecting for concentrations of at least 0.29 wt.% where G' increases gradually with angular frequency. This slight increase in the moduli is common for weak physically cross-linked gels [41]. For the higher concentration samples a minimum in G'' is apparent across the tested frequency range. This minimum has been related to the viscous relaxations which occur between the low and high frequencies: at low frequency, the fibres undergo glasslike rearrangement; at high frequency, the contribution of the solvent viscosity is increasingly important [42].

The thixotropic behaviour of the TOCNF gels was tested through a step strain test. The strain is varied by setting the strain (at constant frequency) either within the LVR region or outside. Similar to the oscillatory amplitude sweep, when $G' > G''$ the gel is behaving solid-like and vice versa. Fig. 6 shows the self-healing behaviour of a 1 wt.% nanocellulose gel. At low strain (0.1%), the gel is acting more solid-like. But once the strain (10%) is increased past the yield point, the gel immediately responds and flows in a viscous manner. Gel behaviour is reversible and changes between elastic-dominated and viscous-dominated regimes instantaneously.

4. Discussion

The discussion is divided into two sections: (1) the effect of pH and ionic strength (electrostatic stabilisation) and (2) the effect of fibre concentration (fibre overlap and entanglement).

4.1. Factors influencing gel stability

4.1.1. Effect of pH

pH affects the level of dissociation of the carboxylic groups, thus changing the density and strength of fibre-fibre interactions. The TOCNF gels produced typically have a pH of 7.4, indicating that most of the pendant groups present are in the sodium carboxylate form as the carboxylic acid pKa is much lower at 4.8. Upon lowering pH, the gel destabilises resulting in the agglomeration of fibres, appearing as semi-translucent aggregates accompanied by the release of water. This was previously observed by Besbes et al. [43] wherein the transmittance of the nanocellulose gels decreased drastically at lower pH indicating fibre agglomeration and destabilisation of the gels. The protonation of the carboxylic groups at low pH decreases the surface potential and electrostatic repulsion allowing the fibres to come in closer contact [44], as shown by the increase in fibres compaction (Fig. 2A). This is likely a result of Van der Waals forces becoming dominant when insufficient charge repulsion is present between the fibres. Another consequence of low pH is the release of water from the gel (Fig. 2A). The change in the counter-ion group from a Na^+ to H^+ drastically decreases the individual fibre and network swelling of TEMPO-oxidised nanocellulose [38]. These evidences prove that electrostatic stabilisation of the ionised COO^- groups conferred by the

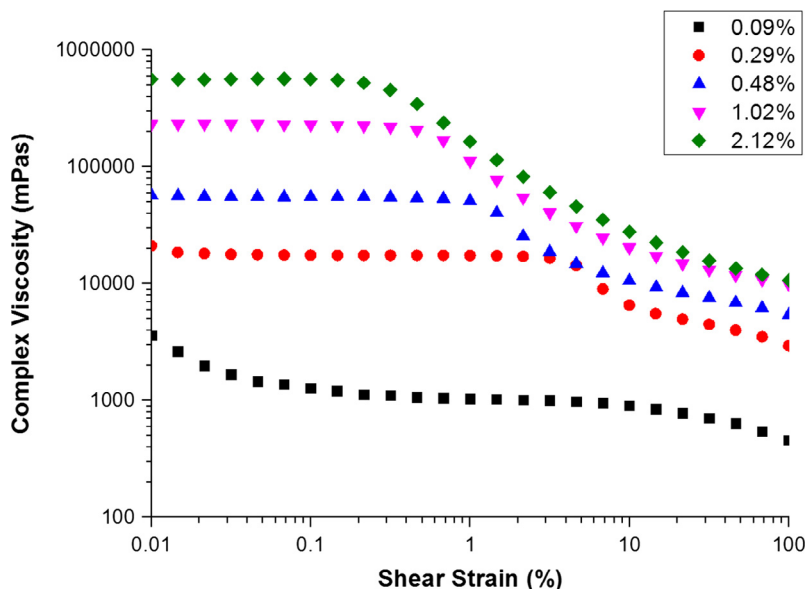


Fig. 3. Complex viscosity profile of shear-thinning TEMPO-oxidised cellulose nanofibre gels at various concentrations derived from dynamic strain sweep measurements (25 °C). A yield point is clearly evident for fibre concentrations of 0.29% and above.

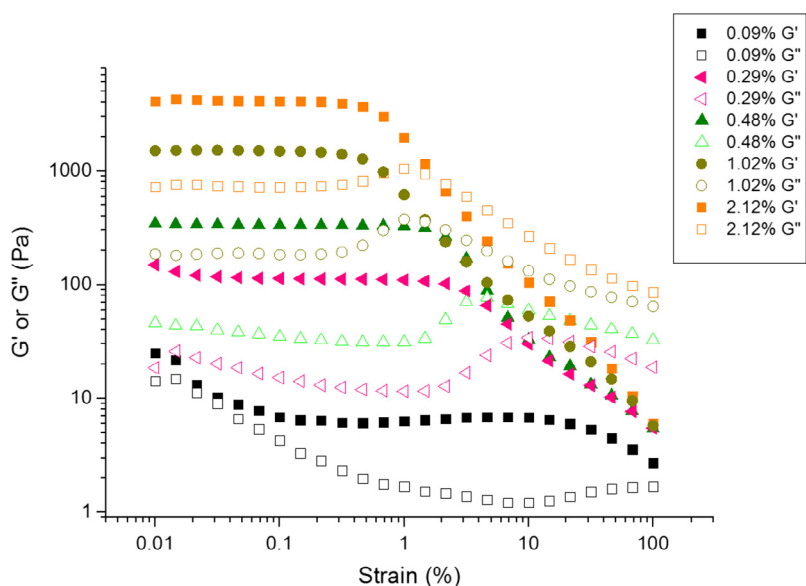


Fig. 4. Viscoelastic properties of TEMPO-oxidised cellulose nanofibre gels at different fibre concentrations: dynamic strain sweep (25 °C) at a frequency of 1 Hz. Filled symbols indicate elastic moduli whereas unfilled symbols indicate loss moduli.

TEMPO-oxidised cellulose nanofibres govern gel stability and formation.

4.1.2. Effect of ionic strength

Salt addition also causes the gel to release water, however not to the same extent as pH (Fig. 2B). Increasing the salt concentration reduces the electrical double layer, which causes an imbalance of the attractive and repulsive forces required for a stable colloid. The double layer thickness is estimated as a function of ionic strength with the Gouy-Chapman equation (Fig. 7). The double layer thickness (1 exponential or 63% decay) ranging from 1.2 to 3.2 nm is similar in magnitude to the diameter of the nanofibers (3–4 nm) [8,10]. Hence, for TEMPO-oxidised nanocellulose fibres, a charge is required in order to form stable network gels.

There is divergence in opinion regarding the effect of ionic strength on the rheological properties of cellulose suspensions.

Some studies claimed that the addition of monovalent salts (e.g. NaCl) to cellulose suspensions can increase both flow (viscosity) and dynamic (G' and G'') rheological properties [45,46]. These microfibrillated cellulose solutions studied were not carboxylated (bearing only OH- groups), which could potentially be a different regime. Both studies linked the increase in rheological properties to the enhanced screening of electrostatic repulsion leading to improved H-bonding between cellulose microfibrils. However, in these studies the microfibrillated cellulose suspensions were not surface modified (only containing OH- groups); hence, the increase in ionic strength allows improved H-bonding between the cellulose microfibrils which results in increased rheological properties. Other studies reported the opposite effect – a decreased viscosity with an increase in ionic strength [26,47,48], however the main difference is these fibres had polarizable groups (carboxylated or carboxymethylated). Carboxylate (~ -75 mV) and car-

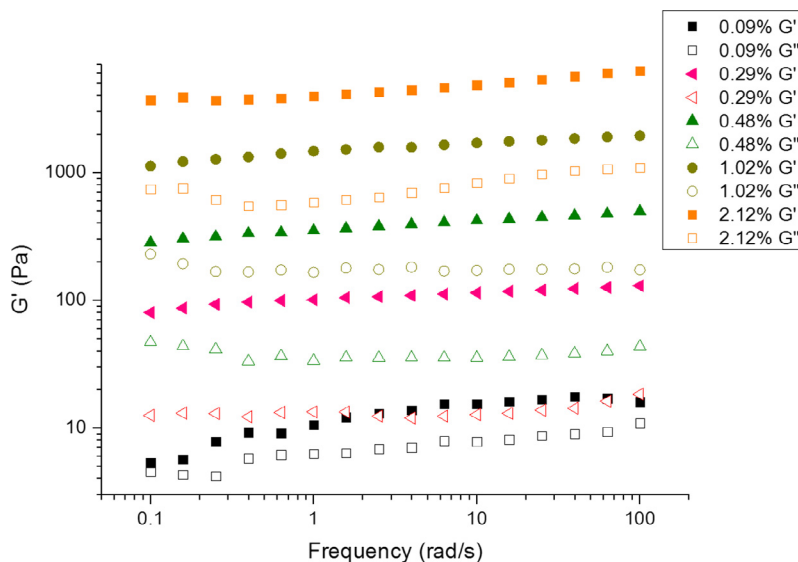


Fig. 5. Viscoelastic properties of TEMPO-oxidised cellulose nanofibre gels as at different fibre concentrations: dynamic frequency sweep (25 °C) at 0.1% strain.

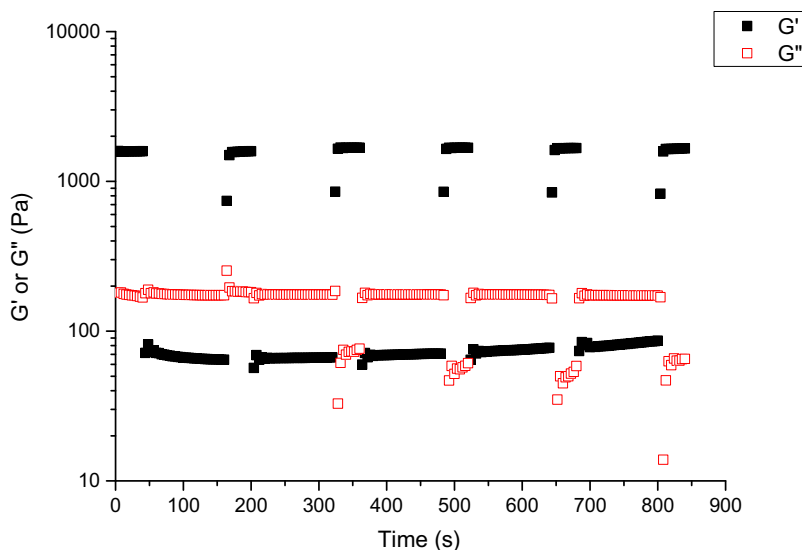


Fig. 6. Rheological properties of 1 wt.% TEMPO-oxidised cellulose nanofibre gel in a step strain test: strain has been varied between 0.1% and 10% at constant 1 Hz and 25 °C for 5 cycles.

boxymethyl groups ($\sim 590 \mu\text{eq/g}$) have a higher surface potential than the hydroxyl groups ($\sim -25 \text{ mV}$) on nanocellulose [8,48,49] leading to higher electrostatic repulsive force between fibres and a different form of fibre-fibre interaction. The screening of these forces results in the collapse of the existing fibre network leading to decreased gel strength properties, as reported.

4.2. Factors governing gel formation and behaviour

4.2.1. Effect of fibre concentration

We utilised rheology to understand the effect of TEMPO-oxidised cellulose nanofibre (TOCNF) concentration on the formation of gel network and its bulk properties. The oscillatory frequency sweep quantifies the gel consistency, which we anticipate is dominated by fibre-fibre interactions, whereas the oscillatory strain sweep characterises bulk flow properties which are dominated by viscosity.

At the lowest concentration (0.09 wt.%), fibres interact very weakly and possess relative motion. Gels at this concentration exhibit a transitional behaviour without strong evidence of material yielding (i.e. no linear viscoelastic region, LVR). Upon increasing the fibre concentration to 0.29 wt.%, the fibres are sufficiently interacting to demonstrate a well-defined LVR with a clear yielding behaviour (as shown in the strain sweep and complex viscosity as a function of strain). Gels containing at least 0.48 wt.% possess a stronger network, as evidenced by higher zero-shear viscosity and by higher G' values. The increase in entanglements at these concentrations also means that the network is becoming less flexible as shown by the yielding of the gels at lower strains.

The formation of the fibre network can also be observed through the evolution of the viscosity profile at increasing concentrations. Cellulose suspensions, whether nano- or micro-fibrillated, are known for their shear-thinning behaviour as the individual fibres can rearrange following the direction of shear. At a sufficient fibre concentration (0.29 wt.% and above), the com-

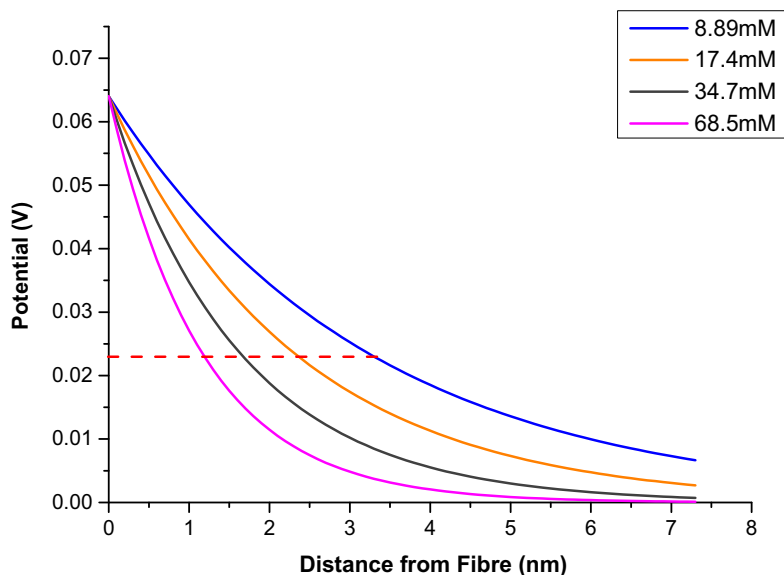


Fig. 7. Effect of ionic strength on the electrical double layer of TOCNF fibres estimated from the Gouy-Chapman equation (reference pH of original gel: 7.4). Dashed line indicates 63% decrease in surface charge corresponding to decreased double layer thickness at increased ionic strength.

plex viscosity demonstrates two shear-thinning regimes of the gel separated by a region of weaker strain dependence. This behaviour was also observed for other forms of nanocellulose [46,50–52]. In microfibrillated cellulose, a plateau region was seen, related to a transitional structure which exists between low and high shear structures. At low shear rates, nanofibres orient along the shear direction causing a decrease in viscosity. Upon reaching the critical shear strain (transition region), the low shear structure breaks down causing an increase in the floc size pre-empting the formation of a new high shear structure. Past this critical strain range, these large flocs are broken into smaller flocs which can move relative to each other [46,50–52].

This transformational behaviour was showed in TOCNF systems by birefringence [33]. TOCNFs re-orient accordingly to shear to produce intermediate structures. Provided that there is enough fibre to make a transitional structure, then and only then a viscosity plateau is reached. This indicates that at 0.09 wt.%, the gel does not possess enough fibre to exhibit this plateau behaviour. However, in more concentrated gels (>2 wt.%), we observe a change in the behaviour of the plateau itself. The plateau is extended and in the second shear-thinning stage the viscosity gradient decreases compared to the lower concentrations (0.29–1 wt.%). This reveals that larger flocs are formed which hinders movement of the gel.

The transitional behaviour highlighted in 0.09 wt.% is also validated by estimating the average number of contact points per fibre through the Crowding Factor Theory [53]. The crowding factor N is defined as the number of fibres present in a sphere wherein the diameter of the sphere is equal to the length of the fibre. The crowding factor (N) can be defined and calculated with the following equations:

$$N = \frac{2}{3} C_v \left(\frac{L}{d} \right)^2 \quad (2)$$

$$N \cong \frac{4\pi n_c^3}{3(n_c - 1)} \quad (3)$$

$$N \cong 4n_c^2 \quad (4)$$

where C_v is the fibre concentration by volume, L and d are the fibre average length and diameter, respectively, and n_c is the number of

contact points per fibre. A minimum n_c of 3 is required to have sufficient contact in order to sustain a network.

At this critical concentration of 0.09 wt.%, $63 \leq N \leq 125$ by estimating fibre length range between 1000 nm and 1400 nm (DLS measurements) and an average diameter of 2.5 nm (from AFM measurement). Assuming a constraint of $n_c \gg 1$ (Simplifying Eqs. (3) to (4)), the estimated number of contact points per fibre lies between $3.98 \leq n_c \leq 5.58$. This indicates that the fibres possess slightly higher than the minimum contact points required for stable network formation and have restricted relative motion resulting into the observed rheological values ($G' > G''$ in frequency sweep). These are characteristics of a gel.

We also investigated the effect of cyclical stress on the 1 wt.% nanocellulose gel to quantify stress relaxation and network recovery behaviour. This was evaluated via a step strain test. The thixotropy of TOCNF gels is due to the non-covalent physical bonding with surrounding fibres. The gels respond to changes in strains as the fibres re-assemble, quickly reforming the gel. On all high strain intervals, the gels possess a viscous dominant behaviour ($G'' > G'$) with both G' and G'' showing reproducible values throughout the test. At low strain intervals, the elastic-dominated behaviour of gel allows quick re-formation; however some degradation in G'' is observed. This hysteretic dependence of G'' may indicate overall structuring of the fibres during the test, or a consolidation of the fibre network during the measurement that results in different viscous dissipation of the gel at lower strains.

5. Conclusion

TEMPO-mediated oxidation is an efficient oxidation process for producing cellulose nanofibres of a small diameter (2–5 nm) [8,10] and high surface charge (COOH). In aqueous suspensions, these elongated nanofibres colloids form cellulosic gels above a critical concentration. Most previous studies on TEMPO-oxidised cellulose nanofibres (TOCNFs) have focussed on the rheological properties, aspect ratio quantification, and production from different substrates or its usability for various applications [25–27,43]. Very few- if any - have analysed cellulose nanofibres in terms of colloidal and interfacial chemistry [24,44]. In this study, we analysed the gelation and colloidal stability of TEMPO-oxidised cellulose nanofibres (TOCNF) by investigating the effect of concentration, pH, and salt content on rheology from a colloids and interfacial

perspective. Gel rheology is examined in terms of nanofiber fibre stability, surface charge (pH) and double layer thickness (NaCl). TOCNFs are elongated and flexible nanofibres forming entangled polymer solutions at low concentrations which transition to gels at higher nanofibre concentrations. This is evidenced by the transition at 0.1 wt.% as measured by rheology and correlation with network theory (Crowding factor). pH and salt strongly influence the colloidal stability of the gels and water is released as the gel collapses. The protonation of the carboxylate groups via the reduction in pH led to a lower surface charge and reduced the amount of water bound to the nanofibers. Increasing ionic strength via salt addition induces charge shielding by compression of the electrical double layer between adjacent fibres, also leading to water release. TOCNFs are colloidal gels- interacting colloidal suspensions of elongated flexible charged particles. The stability of the nanofibres results from the overlap and entanglement of the high aspect ratio fibres combined with electrostatic stabilisation of the pendant COO⁻ groups. Relating the mechanism of TOCNF gel formation to the well-established colloid and interface science enables specific applications in food, biomedical and as rheology modifier to be efficiently engineered from first principles.

Acknowledgments

This work was funded by the ARC Bioprocessing Advance Manufacturing Industry Research Transformation Hub IH13100016, Visy, Norske Skog, Orora, CHH/Oji Paper, and Australian Paper and Circa. Many thanks to Australian Paper for providing the pulp.

References

- [1] D. Klemm et al., Cellulose: fascinating biopolymer and sustainable raw material, *Angewandte Chemie Internat. Edit.* 44 (22) (2005) 3358–3393.
- [2] A. Dufresne, *Nanocellulose From Nature to High Performance Tailored Materials*, 2012: De Gruyter.
- [3] N. Lin, A. Dufresne, *Nanocellulose in biomedicine: current status and future prospect*, *Eur. Polymer J.* 59 (2014) 302–325.
- [4] S. Varanasi, R. He, W. Batchelor, Estimation of cellulose nanofibre aspect ratio from measurements of fibre suspension gel point, *Cellulose* 20 (4) (2013) 1885–1896.
- [5] L. Zhang et al., Effect of cellulose nanofiber dimensions on sheet forming through filtration, *Cellulose* 19 (2) (2012) 561–574.
- [6] T. Saito et al., Cellulose nanofibers prepared by TEMPO-Mediated oxidation of native cellulose, *Biomacromol* 8 (8) (2007) 2485–2491.
- [7] T. Saito, A. Isogai, TEMPO-mediated oxidation of native cellulose. The effect of oxidation conditions on chemical and crystal structures of the water-insoluble fractions, *Biomacromol* 5 (5) (2004) 1983–1989.
- [8] A. Isogai, T. Saito, H. Fukuzumi, TEMPO-oxidized cellulose nanofibers, *Nanoscale* 3 (1) (2011) 71–85.
- [9] O. Nechyporchuk, M.N. Belgacem, F. Pignon, Current progress in rheology of cellulose nanofibril suspensions, *Biomacromol* 17 (7) (2016) 2311–2320.
- [10] H. Fukuzumi et al., Transparent and high gas barrier films of cellulose nanofibers prepared by TEMPO-mediated oxidation, *Biomacromol* 10 (1) (2009) 162–165.
- [11] Q. Li et al., Nanocellulose life cycle assessment, *ACS Sustain. Chem. Eng.* 1 (8) (2013) 919–928.
- [12] R. Weishaupt et al., TEMPO-oxidized nanofibrillated cellulose as a high density carrier for bioactive molecules, *Biomacromol* 16 (11) (2015) 3640–3650.
- [13] A. Rees et al., 3D Bioprinting of carboxymethylated-periodate oxidized nanocellulose constructs for wound dressing applications, *BioMed Res. Internat.* 2015 (2015) 7.
- [14] N.E. Zander et al., Metal cation cross-linked nanocellulose hydrogels as tissue engineering substrates, *ACS Appl. Mater. Interfaces.* 6(21) (2014) 18502–18510.
- [15] J. Cheng, M. Park, J. Hyun, Thermoresponsive hybrid hydrogel of oxidized nanocellulose using a polypeptide crosslinker, *Cellulose* 21 (3) (2014) 1699–1708.
- [16] M. Park, D. Lee, J. Hyun, Nanocellulose-alginate hydrogel for cell encapsulation, *Carbohydr. Polym.* 116 (2015) 223–228.
- [17] M. Bulota, M. Hughes, Toughening mechanisms in poly(lactic) acid reinforced with TEMPO-oxidized cellulose, *J. Mater. Sci.* 47 (14) (2012) 5517–5523.
- [18] S. Fujisawa et al., Superior reinforcement effect of TEMPO-oxidized cellulose nanofibrils in polystyrene matrix: optical, thermal, and mechanical studies, *Biomacromol* 13 (7) (2012) 2188–2194.
- [19] M. Hakalahti et al., Effect of interfibrillar PVA bridging on water stability and mechanical properties of TEMPO/NaClO₂ oxidized cellulosic nanofibril films, *Carbohydr. Polym.* 126 (2015) 78–82.
- [20] T. Saito, A. Isogai, Wet strength improvement of TEMPO-oxidized cellulose sheets prepared with cationic polymers, *Ind. Eng. Chem. Res.* 46 (3) (2007) 773–780.
- [21] K. Dimic-Misic, P.A.C. Gane, J. Paltakari, Micro- and nanofibrillated cellulose as a rheology modifier additive in CMC-containing pigment-coating formulations, *Ind. Eng. Chem. Res.* 52 (45) (2013) 16066–16083.
- [22] X. Sun et al., Cellulose nanofibers as a modifier for rheology, curing and mechanical performance of oil well cement, *Sci. Rep.* 6 (2016) 31654.
- [23] F. Jiang, Y.-L. Hsieh, Super water absorbing and shape memory nanocellulose aerogels from TEMPO-oxidized cellulose nanofibrils via cyclic freezing-thawing, *J. Mater. Chem. A* 2 (2) (2014) 350–359.
- [24] I. Usov, Understanding nanocellulose chirality and structure-properties relationship at the single fibril level, *Nat Commun.* (2015) 6.
- [25] D. Ishii, T. Saito, A. Isogai, Viscoelastic evaluation of average length of cellulose nanofibers prepared by TEMPO-mediated oxidation, *Biomacromol* 12 (3) (2011) 548–550.
- [26] L. Jowkarderis, T.G.M. van de Ven, Intrinsic viscosity of aqueous suspensions of cellulose nanofibrils, *Cellulose* 21 (4) (2014) 2511–2517.
- [27] L. Jowkarderis, T.G.M. van de Ven, Rheology of semi-dilute suspensions of carboxylated cellulose nanofibrils, *Carbohydr. Polym.* 123 (2015) 416–423.
- [28] D.A. Rees, W.E. Scott, Polysaccharide conformation, Part VI. Computer model-building for linear and branched pyranoglycans. Correlations with biological function. Preliminary assessment of inter-residue forces in aqueous solution, Further interpretation of optical rotation in terms of chain conformation, *J. Chem. Soc. B: Phys. Organ.* 1971 0 p. 469–79.
- [29] L. Li, Thermal gelation of methylcellulose in water: scaling and thermoreversibility, *Macromolecules* 35 (15) (2002) 5990–5998.
- [30] K. Bekkour, D. Sun-Waterhouse, S.S. Wadhwa, Rheological properties and cloud point of aqueous carboxymethyl cellulose dispersions as modified by high or low methoxyl pectin, *Food Res. Int.* 66 (2014) 247–256.
- [31] A. Benslimane et al., Thermal gelation properties of carboxymethyl cellulose and bentonite-carboxymethyl cellulose dispersions: rheological considerations, *Appl. Clay Sci.* 132 (2016) 702–710.
- [32] Y. Fang et al., Multiple steps and critical behaviors of the binding of calcium to alginate, *J. Phys. Chem. B* 111 (10) (2007) 2456–2462.
- [33] E. Lasseguette, D. Roux, Y. Nishiyama, Rheological properties of microfibrillar suspension of TEMPO-oxidized pulp, *Cellulose* 15 (3) (2008) 425–433.
- [34] T. Saito et al., Self-aligned integration of native cellulose nanofibrils towards producing diverse bulk materials, *Soft Matter* 7 (19) (2011) 8804–8809.
- [35] H. Dong et al., Cation-induced hydrogels of cellulose nanofibrils with tunable moduli, *Biomacromol* 14 (9) (2013) 3338–3345.
- [36] A. Fernandez-Nieves, A.M. Puertas, Rheology of Soft Materials, in *Fluids, Colloids and Soft Materials*, H.M. Wyss, Editor. 2016, John Wiley & Sons, Inc. p. 149–163.
- [37] R. Shinoda et al., Relationship between length and degree of polymerization of TEMPO-oxidized cellulose nanofibrils, *Biomacromol* 13 (3) (2012) 842–849.
- [38] T.C. Maloney, Network swelling of TEMPO-oxidized nanocellulose, in *Holzforchung*, 2015. p. 207.
- [39] I. Besbes, S. Alila, S. Boufi, Nanofibrillated cellulose from TEMPO-oxidized eucalyptus fibres: effect of the carboxyl content, *Carbohydr. Polym.* 84 (3) (2011) 975–983.
- [40] T. Moberg et al., Rheological properties of nanocellulose suspensions: effects of fibril/particle dimensions and surface characteristics, *Cellulose* 24 (6) (2017) 2499–2510.
- [41] R. Lapasin, Rheological Characterization of Hydrogels, in *Polysaccharide Hydrogels: Characterization and Biomedical Applications*, P. Matricardi, F. Alhaique, and T. Coviello, Editors. 2016, CRC Press. p. 96–97.
- [42] T.G. Mason et al., Osmotic pressure and viscoelastic shear moduli of concentrated emulsions, *Phys. Rev. E* 56 (3) (1997) 3150–3166.
- [43] I. Besbes, M.R. Vilar, S. Boufi, Nanofibrillated cellulose from Alfa, Eucalyptus and pine fibres: preparation, characteristics and reinforcing potential, *Carbohydr. Polym.* 86 (3) (2011) 1198–1206.
- [44] A.B. Fall et al., Colloidal stability of aqueous nanofibrillated cellulose dispersions, *Langmuir* 27 (18) (2011) 11332–11338.
- [45] M.P. Lowys, J. Desbrières, M. Rinaudo, Rheological characterization of cellulosic microfibril suspensions. Role of polymeric additives, *Food Hydrocolloids* 15 (1) (2001) 25–32.
- [46] E. Saarikoski et al., Flocculated flow of microfibrillated cellulose water suspensions: an imaging approach for characterisation of rheological behaviour, *Cellulose* 19 (3) (2012) 647–659.
- [47] R. Tanaka et al., Determination of nanocellulose fibril length by shear viscosity measurement, *Cellulose* 21 (3) (2014) 1581–1589.
- [48] A. Naderi, T. Lindström, T. Pettersson, The state of carboxymethylated nanofibrils after homogenization-aided dilution from concentrated suspensions: a rheological perspective, *Cellulose* 21 (4) (2014) 2357–2368.
- [49] P. Raj et al., Effect of cationic polyacrylamide on the processing and properties of nanocellulose films, *J. Colloid Interface Sci.* 447 (2015) 113–119.
- [50] G. Agoda-Tandjawa et al., Rheological characterization of microfibrillated cellulose suspensions after freezing, *Carbohydr. Polym.* 80 (3) (2010) 677–686.
- [51] M. Iotti et al., Rheological studies of microfibrillar cellulose water dispersions, *J. Polym. Environ.* 19 (1) (2011) 137–145.
- [52] A. Karppinen et al., Flocculation of microfibrillated cellulose in shear flow, *Cellulose* 19 (6) (2012) 1807–1819.
- [53] R.J. Kerekes, C.J. Schell, Characterization of fibre flocculation regimes by a crowding factor, *J. Pulp Pap. Sci.* 18 (1) (1992) J32–J38.